Antibacterial Surfaces With Activity Against Antimicrobial Resistant Bacterial Pathogens and Endospores

Sandeep K. Sehmi[1, 2, 3],† Claudio Lourenco[1, 2]†, Khaled Alkhuder[1], Sebastian D. Pike[5], Sacha Noimark[4], Charlotte K. Williams[6], Milo S.P. Shaffer[5], Ivan P. Parkin[2]*, Alexander J. MacRobert[3]* and Elaine Allan[1]*

[1]Division of Microbial Disease, UCL Eastman Dental Institute, University College London, 256 Gray's Inn Road, London, WC1X 8LD, UK.

[2]Materials Chemistry Research Centre, Department of Chemistry, University College London, 20 Gordon Street, London, WC1H 0AJ, UK.

[3]UCL Division of Surgery and Interventional Science, University College London, Royal Free Campus, Rowland Hill Street, London, NW3 2PF, UK.

[4]Department of Medical Physics and Biomedical Engineering, University College London, Gower Street, London, WC1E 6BT, UK.

[5]Department of Chemistry, Imperial College London, Imperial College Road, London, SW7 2AZ, UK.

[6]Chemistry Research Laboratory, University of Oxford, 12 Mansfield Road, Oxford, OX1 3TA.

†joint first authors

*corresponding authors

E-mails: e.allan@ucl.ac.uk, a.macrobert@ucl.ac.uk, i.p.parkin@ucl.ac.uk

Hospital-acquired bacterial infections are a significant burden on healthcare systems worldwide causing increased duration of hospital stays and prolonged patient suffering. We show that polyurethane containing crystal violet (CV) and 3-4 nm zinc oxide nanoparticles (ZnO NPs) possesses excellent bactericidal activity against hospital-acquired pathogens including multidrug resistant *Escherichia coli*, *Pseudomonas aeruginosa,* methicillin-resistant *Staphylococcus aureus* (MRSA) and even against highly-resistant endospores of *Clostridioides (Clostridium) difficile*. Importantly, we used clinical isolates of bacterial strains, a protocol to mimic the environmental conditions of a real exposure in the healthcare setting and low light intensity equivalent to that encountered in UK hospitals (~500 lux). Our data shows that ZnO NPs enhance the photobactericidal activity of CV under

low intensity light even with short exposure times and we show that this involves both Type I and Type II photochemical pathways. Interestingly, polyurethane containing ZnO NPs alone showed significant bactericidal activity in the dark against one strain of *E. coli* indicating that the NPs possess both light-activated synergistic activity with CV and inherent bactericidal activity that is independent of light. These new antibacterial polymers are potentially useful in healthcare faciilties to reduce the transmission of pathogens between people and the environment.

Keywords

Crystal violet, zinc oxide nanoparticles**,** photo-active, antibacterial surface, antimicrobial resistance**,**

The antibacterial activity of zinc oxide nanoparticles (ZnO NPs) has attracted much attention in recent years due to the multi-functionality and biocompatibility of ZnO when synthesised with nanometre range diameters. ZnO NPs have shown selective toxicity towards bacteria and minimal effects on mammalian cells.[1] They have many potential applications and are already used in the food-packaging industry as antibacterial agents against food-borne pathogens.[2] ZnO has a wide band gap (3.3 eV)[3] and is used as a UV protector in cosmetics as it possesses high optical absorption in the UV region.[4] The mechanism of antibacterial action of ZnO NPs is unclear, although some studies suggest that their main activity comprises Zn^{2+}-mediated disruption to the bacterial cell membrane.[5] Another possible mechanism of action is the induction of reactive oxygen species (ROS), including hydrogen peroxide (H_2O_2), which are harmful to bacterial cells.[6] Several reports suggest that when activated by visible or UV light, ZnO NPs can generate ROS including OH^-, H_2O_2, and $^1O_2$.[2–5]

Hospital-acquired infections (HAIs) are a major threat to patients, visitors and healthcare workers, causing an estimated 5000 deaths per year in the UK.[7] In addition, they pose a significant economic burden on healthcare systems world-wide and are a particular risk for the elderly, children and patients with compromised immune systems.[8] As a result of the increasing incidence of HAIs, which are often caused by multidrug resistant pathogens, the development of novel antibacterial strategies is urgent.[9] Infections caused by methicillin-resistant *Staphylococcus aureus* (MRSA) and carbapenem-resistant Enterobacteriaceae (CRE) infections are two of the major challenges currently faced by healthcare facilities as these bacteria are resistant to most currently available antibiotics.[10] The overuse of antibiotic treatment itself presents problems in the healthcare environment, however, as it increases the risk of hospital-associated diarrhoea due to infection with *Clostridioides (Clostridium) difficile*.[11] Patients with *C. difficile* infection shed endospores in their feces which are transmitted to

other patients via frequently touched surfaces. These spores are able to persist in the environment for long time periods and if ingested by patients whose protective microbiota has been disrupted by broad spectrum antibiotics, they may germinate and produce toxins resulting in diarrhoeal disease.[11,12]

Antibacterial surfaces are effective in decreasing the incidence of HAIs by reducing the spread of bacteria between patients, staff and frequently-touched surfaces such as call buttons, telephones, keyboards and bed rails.[13] For surfaces to be effective at reducing bacterial transmission, they need to be self-sterilising and durable. One approach is to use non-toxic photosensitising agents which can be coated onto surfaces.[14–24] Upon light activation, these photo-activated antimicrobial surfaces can generate cytotoxic ROS *via* a process known as photodynamic therapy (PDT).[14–24] PDT can occur through two main pathways: (i) Type I (electron transfer) to produce superoxide anion radicals and/or (ii) Type II (energy transfer) to produce singlet oxygen ($^1O_2$).[25] The superoxide radical anions can then undergo dismutation to generate hydrogen peroxide and then hydroxyl radicals via the Fenton process. PDT is an attractive strategy for treating bacterial infections since it has multiple targets in the bacterial cell thus reducing the likelihood of resistance developing.[26,27]

Typical photosensitisers such as methylene blue, toluidine blue O and crystal violet (CV), can be incorporated into polymers and tested against bacteria following white light activation and in the dark. Previous studies carried out by our research group have shown the effectiveness of incorporated photosensitisers for medical devices and antibacterial surface coatings.[14–24] Additionally, we have found that incorporating nanoparticles (e.g. Au, Cu, TiO_2, MgO, ZnO) together with the photosensitiser can significantly enhance the bactericidal activity.[14,15,17,19–23] We have also shown that the degree of synergy observed is dependent on the size of the nanoparticles and the light intensity used for activation.[6,14,15,17,19–22,26,27] In previous studies,[14,28] we found that small ZnO nanoparticles are particularly effective; here we synthesised highly soluble, small NPs stabilised by oleate ligands for encapsulation into polyurethane. A limitation of previous work is that microbiological testing was performed on domesticated laboratory strains of bacteria which may no longer be representative. Here, we used a broad range of clinically-relevant Gram-positive and Gram-negative bacterial pathogens including *Pseudomonas aeruginosa,* MRSA and *E. coli* and importantly, we have included both recent clinical isolates expressing multidrug resistance and *C. difficile* endospores which are highly resistant to killing by other means including heat and chemical disinfection.[29,30] In addition, we modified our previous protocol to more closely mimic the environmental conditions of a 'real world' exposure within a hospital environment.

Results and Discussion

In this work, we first synthesised small ZnO nanoparticles (3-4 nm) stabilised by oleate ligands, and subsequently encapsulated them within the polyurethane film. Previous reports have suggested a beneficial effect of using oleate groups in antimicrobial moieties.[28] The oleate-capped ZnO NPs are themselves very soluble in organic solvents making them ideal candidates for the 'swell-encapsulation-shrink' technique utilised here. The particles were prepared by the controlled hydrolysis of an organometallic precursor ($ZnEt_2$) in the presence of 0.2 equivalents of oleic acid (to give a 5:1 metal:ligand ratio).[31] After preparation, the nanoparticles were kept in an inert environment (e.g. under N_2) as evidence shows they may slowly ripen over several months if exposed to atmospheric moisture.[32] The particles were characterised by powder X-ray diffraction and UV-spectroscopy to determine the size of the particles,[33] with freshly prepared samples consistently showing sizes between 3-4 nm. IR spectroscopy confirmed surface coordinated oleate ligands along with surface hydroxide groups[34] (Fig S1). Elemental analysis showed final metal:ligand ratios of 5.3-5.4:1, suggesting a very slight loss of ligand during the nanoparticle synthesis. A Tauc plot measured the band onset of ZnO NPs suspended in toluene, estimating the band gap to be ~3.48 ±0.01 eV (Fig. S7, supporting information).

ZnO NPs were incorporated into 1 cm^2 medical grade polyurethane samples using a simple and easily upscalable, 'swell-encapsulation-shrink' method (described in 1.1.3, supporting information). Once incorporated, ZnO-containing polymer squares were immersed in a 0.001 M aqueous solution of CV in water, to produce a polymer containing both CV and ZnO (CVZnO). The modified polymers were characterised using UV-vis absorbance and X-ray photoelectron spectroscopy (XPS). In the UV-vis spectrum, polyurethane coated with either CV or CVZnO showed an absorbance maximum at λ = 590 nm (Fig. S8), but no characteristic absorption peak for ZnO was observed presumably due to the low concentration of NPs encapsulated. XPS data confirmed that ZnO NPs were encapsulated and localised near the polymer surface (Fig. 1), showing a doublet in the Zn (2p) region indicating the presence of Zn in ZnO. Fig 1(c) shows a cross-sectional SEM image of the modified polymer and no apparent damage is evident such as cracking to the polymer due to the uptake of the dye and the exposure to solvent through incorporation of zinc oxide nanoparticles. Furthermore, SEM showed that there was uniform uptake of the CV in a polymer section with a 0.8 mm depth (Fig. S9).

The photostability of CV- and CVZnO-coated polyurethane samples was examined under a 3880 lux white light source for up to 60 days (Fig. S10). The results from UV-vis spectroscopy indicated that both samples were relatively photostable, even under a light source which is ~19-fold more intense

than that of many hospital wards and corridors (~200 lux).[35,36] Over the 60-day period, the CV-coated polymer showed a 34% reduction in peak maxima compared to 39% for the polymer containing CVZnO, suggesting that these materials are likely to exhibit reasonable long term photostability at the lower light levels typical of hospital wards and corridors. Inductively-coupled plasma-optical emission spectroscopy (ICP–OES) was used to determine if any zinc species leached from the ZnO-incorporated polymer when the films were immersed in water. Modified polymer squares were immersed in distilled water for up to 48 h. Results showed that small amounts of zinc species were leached from the polymer (0.096 ± 0.002 mg/L after 2 h and 1.008 ± 0.006 mg/L after 48 h).

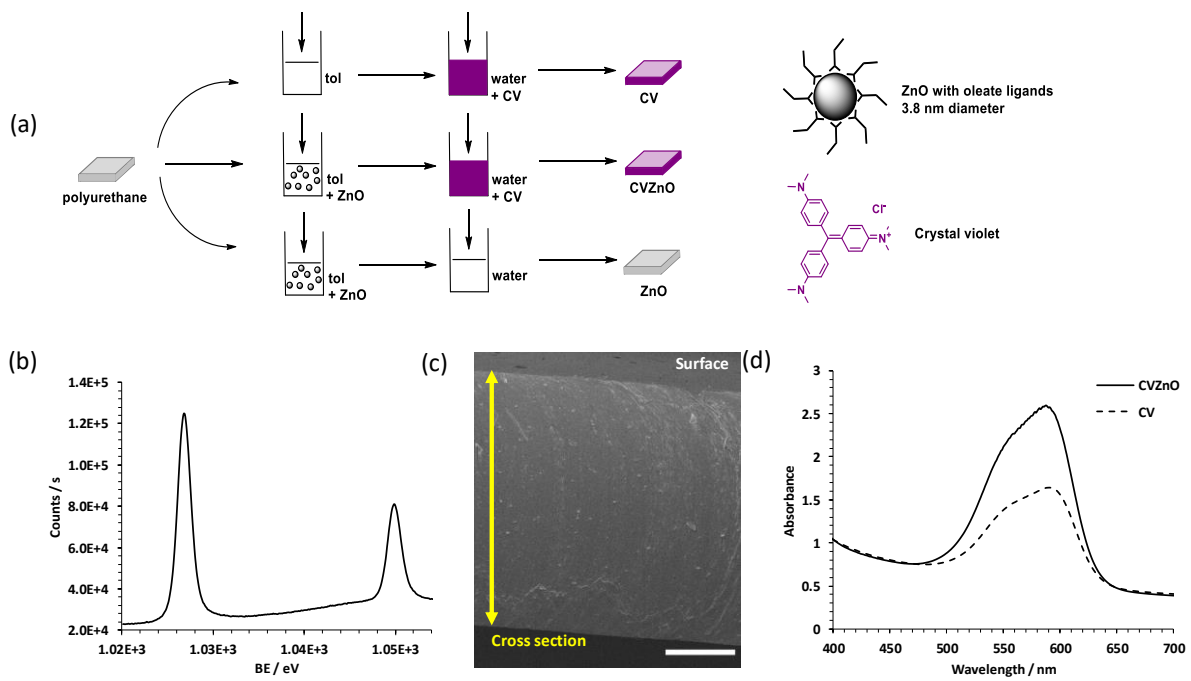

Fig. 1 (a). Schematic of the materials synthesis demonstrating that the control and test samples underwent the same preparation process; (b) overlaid XPS spectra for CVZnO in the Zn(2p) region after 50s of sputtering; (c) SEM side-on image of the ZnO-polyurethane composite mounted on glass slide (bottom of image), scale bar: 200 μm; (d) Uv-vis spectra of crystal violet impregnated polyurethane and crystal violet-ZnO impregnated polyurethane.

The modified polymer samples were tested for antibacterial activity against different bacterial species in the dark and during exposure to ambient laboratory lighting (~500 lux). Samples were exposed to *E. coli* ATCC 25922 for up to 3 h using the protocol described previously.[9] The antibacterial activity of the samples was tested against this bacterium to enable a comparison with previous materials

synthesised in our group.[14,15,17–23] Within only 2 h of white light exposure (Fig. S11), CVZnO reduced the numbers of *E. coli* ATCC 25922 to below the detection limit and ZnO alone caused a ~2 log reduction in bacterial numbers (P = 0.001), whereas there was no significant reduction in bacterial viability on the control material. Even in the dark, after 2 h CVZnO demonstrated highly significant bactericidal activity against this strain of *E. coli* (≥4 log reduction in bacterial numbers) and ZnO alone achieved ~1.7 log reduction (P = 0.001 The antibacterial activity of ZnO alone could be attributed to leaching of Zn^{2+} from the polymer which is taken up by the bacteria

The antibacterial efficacy of the polymers was then tested against other Gram-positive and Gram-negative bacteria (*P. aeruginosa* NTCC 10662, *Staphylococcus aureus* NCTC 13143 (this strain is a representative of epidemic clone EMRSA-16, one of two EMRSA clones which predominate in the UK[29]), a recent clinical isolate of methicillin-resistant *Staphylococcus aureus* (MRSA 4742; obtained from P. Wilson, University College London Hospital), *E. coli* 1030, a strain expressing carbapenemase enzymes which renders the bacterium resistant to the drugs of last resort, the carbapenems; (obtained from J. Wade, King's College Hospital, London) and spores of *C. difficile* 630, a virulent and multidrug-resistant strain isolated from a hospital patient with severe pseudomembraneous colitis[37]. In previous experiments, we have placed the bacterial suspension on to the test polymer and used a coverslip to ensure good contact between the bacteria and the material. Here, in an effort to more closely mimic a natural exposure, the bacterial suspension was simply dropped on to the surface of the polymer and allowed to dry.

Fig. 2 summarises the antibacterial activity of the polymer samples against different hospital-acquired pathogens. The control material and polymer containing ZnO alone did not produce any significant bactericidal activity either in the dark or after white light illumination. Fig. 2(a) shows the bactericidal activity of the polymer samples against *P. aeruginosa* NCTC 10662 following 6 h of incubation in the light and dark. In the dark, CV alone reduced the numbers of *P. aeruginosa* by ~0.6 log whereas the combination of CV and ZnO in the dark was able to reduce the numbers by ~1 log. With 6 h of white light activation, polyurethane containing CV alone resulted in a ~1.3 log reduction in the numbers of *P. aeruginosa* whereas the polymer containing CVZnO reduced bacterial numbers to below the detection limit (≥4 log reduction; P = 0.001). Indeed, within only 4 h of light exposure, CVZnO reduced the number of *P. aeruginosa* by ~2.5 log (data not shown).

The samples were also tested against *S. aureus* NCTC 13143 (Fig. 2(b). After 2 h in the dark, exposure to CVZnO resulted in a ~2.4 log reduction in the numbers of *S. aureus* and with 2 h of light exposure, the numbers of bacteria were reduced to below the detection limit (≥ 4 log; P = 0.001). The test

samples also showed good activity against a recent clinical isolate of MRSA (strain 4742) producing a 3.4 log reduction (P = 0.01) in the bacterial numbers after 2 h of exposure to white light (Fig. S10(c)).

The samples were then tested against *E. coli* 1030, a multidrug-resistant clinical isolate positive for both NDM and OXA-48-like carbapenemase enzymes. CVZnO demonstrated statistically significant bactericidal activity against *E. coli* 1030 in the dark within 4 h (~1.9 log reduction, P = 0.001). Interestingly, in the light, CV alone reduced the numbers of *E. coli* 1030 by ~1.5 log, whereas exposure to the CVZnO-containing polymer reduced the numbers by ~4 log (P = 0.001).

Since a reduction in *C. difficile* spores within healthcare environments is currently a major challenge, we tested the photobactericidal efficacy of our samples against *C. difficile* endospores. No significant sporicidal activity was apparent in the dark. However, following 72 h of white light exposure, the polymer containing CVZnO achieved a further ~1.2 log reduction in the number of spores compared to the control. (P = 0.001; Fig. 2(d) It is not clear why a greater than 1 log reduction in the numbers of *C. difficile* spores apparently occurred on the control polymer. We assume that since no reduction in the spore counts was apparent on the control polymer in the dark, that this was due to reduced recovery of the spores from the surface of the light-exposed material as a result of drying. Whereas the bacterial suspension was still wet on the control polymer incubated in the dark at the end of the period of exposure, the suspension on the surface of the control polymer incubated in the light had dried during the exposure period which presumably resulted in less efficient spore recovery.

The modified polymer samples containing both CVZnO demonstrated highly significant light-activated bactericial activity against all the healthcare-associated pathogens tested (Fig. 2) and even showed good activity against one strain of *E. coli* (ATCC 25922) in the dark (Fig. S10). Polyurethane containing only ZnO NPs also showed some bactericidal activity in the dark against this strain and light-activated synergy with CV (Fig. S10). For all the bacterial species tested, an increase in the antibacterial activity of CV was observed when ZnO NPs were combined implying that the nanoparticles are responsible for enhancing the intrinsic (dark) bactericidal activity of CV itself and and also enhancing the light-activated bactericidal activity of the dye. The activity of the CVZnO polymer against *C. difficile* spores is encouraging since fecal shedding of spores by *C. difficile*-infected patients and contamination of environmental surfaces is the major infection source during hospital outbreaks; thus even a conservative reduction in spore numbers is likely to positively impact on infection control.

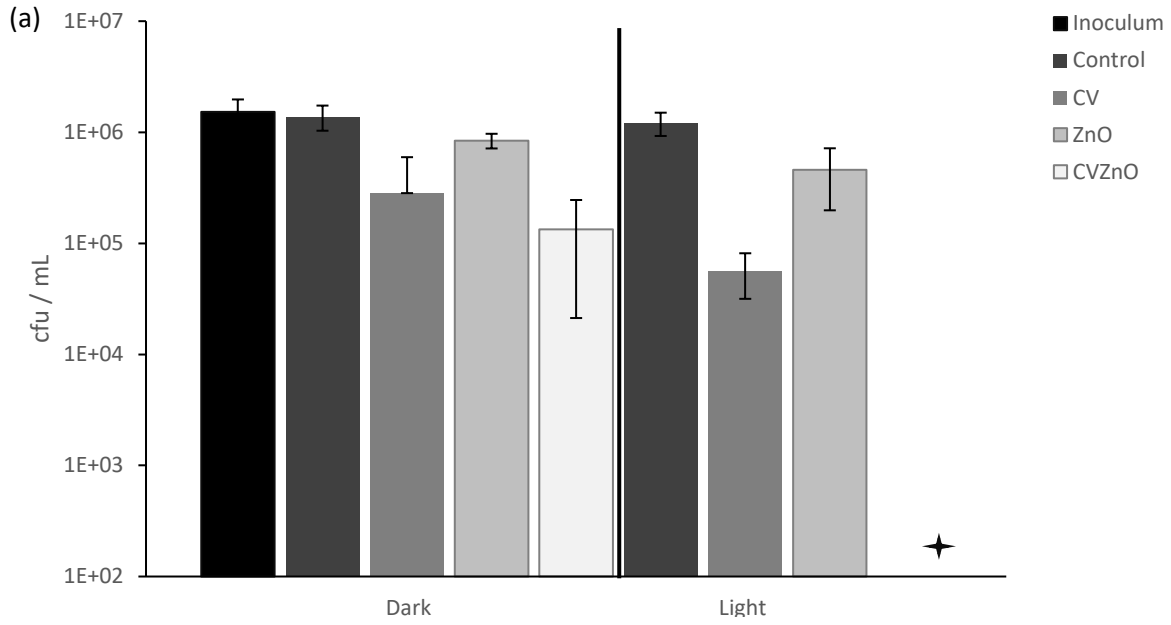
(a)
1E+07
1E+06
1E+05
1E+04
1E+03
1E+02
cfu / mL
Dark
Light
Inoculum
Control
CV
ZnO
CVZnO

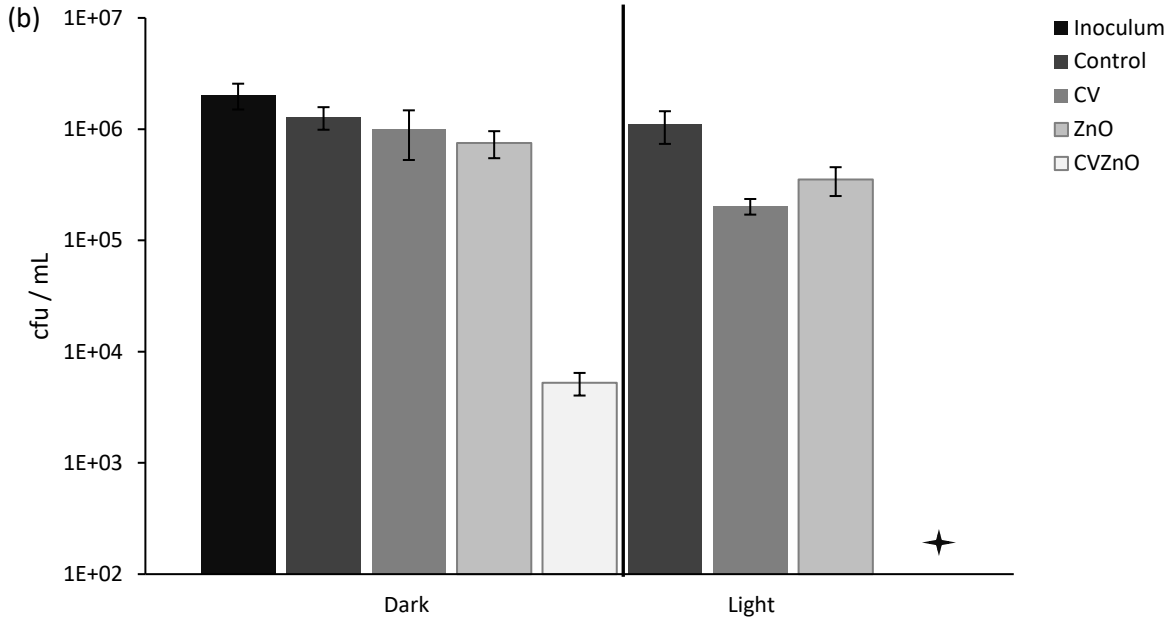
(b)
1E+07
1E+06
1E+05
1E+04
1E+03
1E+02
cfu / mL
Dark
Light
Inoculum
Control
CV
ZnO
CVZnO

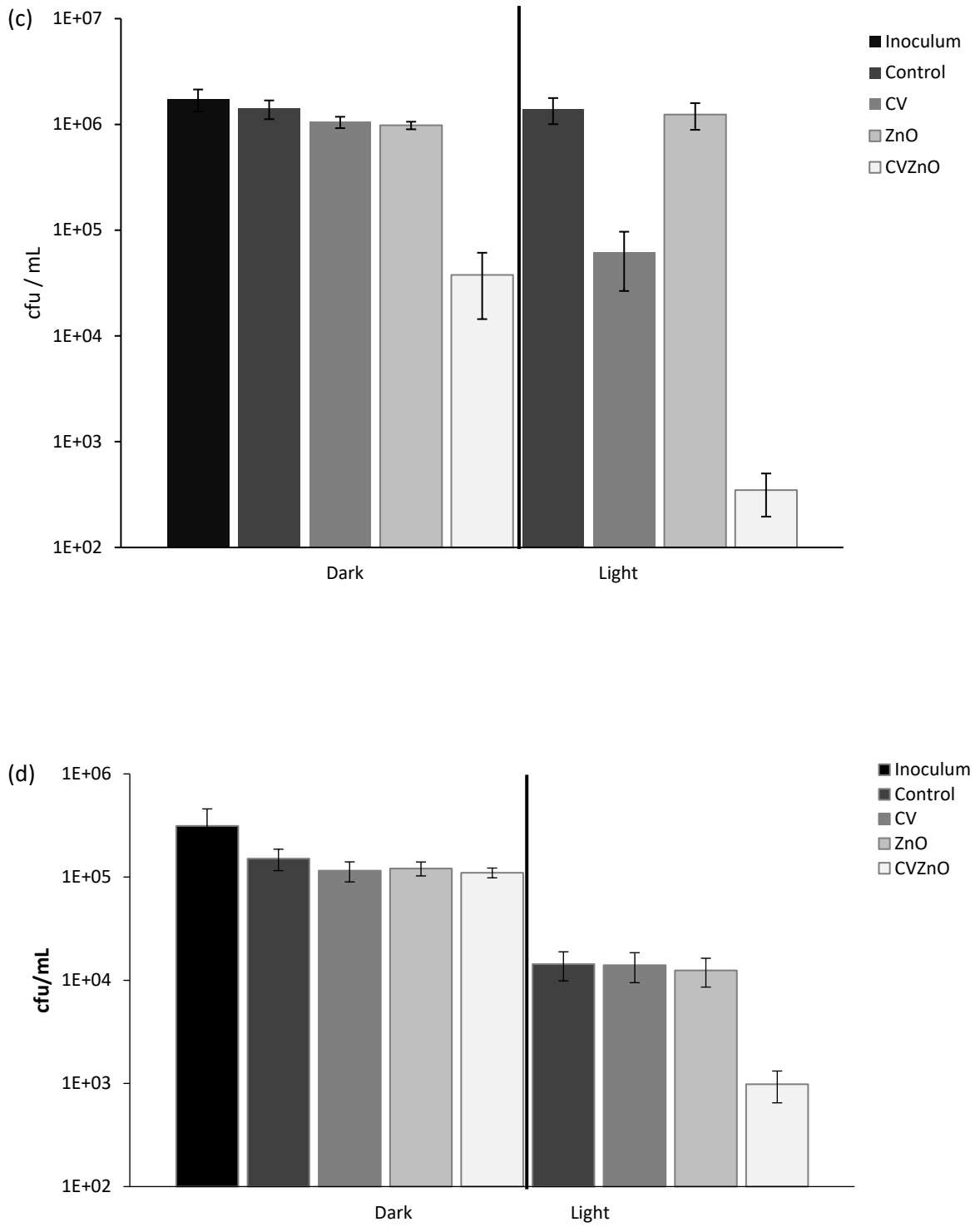

Fig. 2 Viable counts of bacteria after incubation at 20°C on modified polyurethane squares after exposure to standard laboratory white light (500 ± 300 lux) and in the dark: (a) *P. aeruginosa* NTCC 10662 (6 h), (b) *Staphylococcus aureus* NCTC 13143 (2 h), (c) *E. coli* 1030 (4 h) and (d) *C. difficile* 630 spores (72 h). ✦ indicates that the viable count was below the detection limit of 100 cfu/ml. Control is the untreated polymer. In (a), the negative error bar is not displayed for CV alone as the SD is larger than the mean due to the small sample size.

Next we investigated the effect on the bactericidal activity of the polymers when different ligands and different metal:ligand ratios were used for the ZnO NP synthesis. ZnO NPs were synthesised with either oleate ($C_{18}H_{34}O_2$; with a double bond in the organic chain), stearate ($C_{18}H_{36}O_2$; no double bonds) or linoleate ($C_{18}H_{32}O_2$; two double bonds) carboxylate ligands. The structures of these ligands are shown in Fig. S12, supporting information). As shown in Table 1, ZnO capped with an oleate ligand was synthesised again but here a greater metal : ligand ratio was used – i.e. 10:1 compared to 5:1 used previously. Also, stearate and linoleate-capped ZnO (5:1) were synthesised to see if changing the ligand chain would alter the bactericidal properties of the system, as the ligands, in the form of the free acids, are themselves known to possess antibacterial activity.[38–40] The total ZnO surface area of 1 mg of the NPs remained essentially consistent in all cases (Table 1), since particles with less ligand (more ZnO/g) are coincidentally larger in diameter with a lower surface area per particle. Therefore, the swelling solutions were all prepared with 1 mg of ZnO per mL. It is noteworthy that the solubility in organic solvents of these ZnO NPs was reduced compared to the original oleate-capped ZnO NPs (5:1) system. The antibacterial activity of polymer containing the different ligand:metal combinations was assessed using *E. coli* ATCC 25922 after 2 h of standard laboratory white light exposure (~500 lux). The results showed that the bactericidal activity of linoleate- and stearate-capped ZnO was less than the oleate-capped ZnO in the light: the linoleate- and stearate-capped only achieved ~1 log reduction in the numbers of *E. coli* ($P = 0.001$) compared to ≥4 log for the oleate-capped ZnO (Table 1). Linoleate-capped ZnO was the least soluble and did not demonstrate any significant kill in the dark. Stearate-capped ZnO reduced bacterial numbers by ~1 log in the dark ($P = 0.001$) whereas oleate-capped ZnO produced a ≥4 log reduction. Comparing the different ratios of oleate-capped ZnO, the 10:1 ratio was not as effective as the 5:1 ratio presumably because the 10:1 oleate-capped ZnO NPs were bigger in size (Table 1). Within 2 h of white light exposure, the oleate-capped ZnO (10:1) reduced the numbers of *E. coli* by 2 log ($P = 0.001$) and showed no kill in the dark. As reported previously by ourselves and by others, this study confirms that the antibacterial activity of nanoparticles is size dependent.[6,14,15,17–23,41,42]

Table 1. Summary of the nanoparticle surface area and ligand coverage of all ZnO nanoparticles. Approximate diameter calculated from UV spectroscopy (Fig S6). Antibacterial activity of the ligands encapsulated into polyurethane (without CV against *E. coli* ATCC 25922) after 2 h exposure to white light (500 ± 300 lux).

Ligand	*Ratio*	*wt % ligand by elemental analysis (carbon %)*	*Approximate Diameter (nm)*	*ZnO Surface Area of 1 mg*	*Estimated Ligand*	*Antibacterial activity after 2 h*

				of particles (m^2)	*Coverage (% ZnO surface)*	*white light (500 ± 300 lux)*
Oleate	5:1	39	3.8	0.17	95	≥4 log
Oleate	10:1	25.6	4.9	0.16	65	2 log
Stearate	5:1	40	3.6	0.18	93	1 log
Linoleate	5:1	35.2	4.0	0.17	86	1 log

In our previous study using ZnO nanoparticles which were larger than those studied herein, we showed that both Type I and II ROS generating pathways are involved in by studying the effects of ROS inhibitors on bactericidal activity. Likewise Bovis *et al*. showed that both Type I and Type II mechanisms can operate with silicone doped with methylene blue and nanogold.[43]

To investigate the mechanism responsible for the bactericidal activity of the CVZnO-containing polymers, either superoxide dismutase[44] (SOD; 50 U mL^{-1}) was added to the system to remove superoxide anions or L-histidine (1 mM) was included as a singlet oxygen quencher to determine the contribution made by a Type I or Type II photochemical pathway, respectively[14]. SOD or L-histidine was added to the bacterial suspension before exposure to the polymer and the antibacterial activity against *E. coli* ATCC 25922 and *S. aureus* NCTC 13143 was determined in the light and in the dark (data shown in Fig. S13-S14, supporting information). The results indicate that both Type I and Type II mechanistic pathways contribute to the antibacterial activity of CVZnO against both bacteria in the dark and in the light. The results also suggest that the Type I and Type II reactions occur at the same rate as both SOD and histidine reduced the bactericidal activity to a similar extent. Interestingly, the bactericidal activity of polyurethane containing ZnO alone against *E. coli* ATCC 25922 is barely affected by the presence of either inhibitor indicating that the mechanism does not involve the production of superoxide or singlet oxygen (Fig. S14) and may result from leached zinc ions, shown previously to make a minor contribution to antibacterial activity.[28,45]

To confirm the production of singlet oxygen in the CVZnO system under visible light activation, furfuryl alcohol (FFA) and L-ascorbic acid were used separately as singlet oxygen quenchers. Under visible light, the oxidative degradation of FFA[46] showed that a significant amount of singlet oxygen was produced in the photoactivation of CVZnO (Table S2, supporting information) compared to CV alone, and none was produced from the polymer alone or from the polymer containing only ZnO. The increase in singlet oxygen production is partly explained by UV-vis spectroscopy (Fig. S8) which shows that a higher mean concentration(by approximately a factor of two) of CV are incorporated when ZnO is present. In the dark, none of the modified samples caused any diminution of FFA (data not shown). It should be noted

that FFA does not absorb in the visible spectrum and therefore was not deactivated during the experiment.

Using the same microbiological protocol and conditions, L-ascorbic acid (1 mM) was added to the bacterial suspension. CVZnO with L-ascorbic acid resulted in only a ~2 log reduction of *E. coli* ATCC 25922 under white light activation, compared to a reduction of ≥4 log in the absence of the quencher (Fig. S15, supporting information). CV with L-ascorbic acid reduced the bacterial numbers by only ~1 log, compared to a 2 log reduction in the absence of quencher. No change in antibacterial activity was observed in the dark in the presence of quencher. These results suggest that upon white light illumination, chemical quenching of singlet oxygen occurs as it reacts readily with ascorbate, producing hydrogen peroxide.[47] Furthermore, the combination of ZnO and CV produces more singlet oxygen than CV alone, whereas there is no evidence of singlet oxygen production by the polymer containing ZnO alone. It should be noted that L-ascorbic acid is not quenched without white light activation (i.e. dark kill).

We have shown mechanistic evidence for the photochemical pathways occurring within the CVZnO system when exposed to light and in the dark. We have also demonstrated that the combination of the smaller NPs and the oleic acid capping agent results in improved antibacterial activity, in comparison to previous work incorporating ~15 nm ZnO NPs in polyurethane.[14] For the first time, we prepared oleic acid-capped ZnO-incorporated polyurethane surfaces that achieve lethal photosensitisation of *E. coli* ATCC 25922 without a photosensitiser within 2 h (Fig. S10) supporting information). ICP-OES analysis indicated small amounts of zinc leaching from ZnO-incorporated polyurethane within 2 h. Whilst a similar amount of leaching is observed with previously studied dioctylphosphinate (DOPA)-capped ZnO NPs incorporated into polyurethane[28] after 2 h, we note that after 48 h approximately 4x more Zn is leached in the case of oleate-capped ZnO. This suggests the ligand may play some role in the leaching mechanism. Mechanistic studies have shown that the NPs do not produce ROS species on their own but when combined with CV there is greater production of ROS and more significantly, singlet oxygen.

These antibacterial polymers show great promise as potential surfaces in hospitals to reduce the spread of HAIs. Significant bactericidal activity was observed under low intensity lighting and in the dark, proving more effective than other antibacterial systems previously described which used much higher light intensties (above 10,000 lux).[18,20] Additionally, these new bactericidal polymers have demonstrated efficacy against a much higher bacterial load than would occur in a hospital environment; ~1 x 10^5 cfu/cm^{-2} of bacteria used in this investigation compared to an average of 1 x 10^2 cfu/cm^{-2} found in a clinical environment.[18,20,21]

Conclusion

Polyurethane containing crystal violet and 3-4 nm zinc oxide nanoparticles exhibited good bactericidal activity against clinical isolates of multidrug resistant hospital-acquired pathogens including *E. coli*, *P. aeruginosa,* MRSA and even showed activity against the highly-resistant endospores of *C. difficile*. Importantly, activity was apparent with low light intensity equivalent to that encountered in UK hospitals suggesting that these surfaces could potentially contribute to reducing the cycle of transmission of healthcare-associated pathogens between people and the environment. The mechanism of bactericidal activity was shown to involve generation of both superoxide and singlet oxygen in both the light and the dark.

Experimental Section

Synthesis of oleate-capped ZnO nanoparticles: Oleic acid was placed into a Schlenk flask with a stirrer and dried under vacuum. Dry toluene was added to the ligand in a glovebox and then 5 equivalents of diethyl zinc ($ZnEt_2$) was added dropwise to the solution whilst stirring. A 0.4 M solution of water in acetone was added to the mixture to hydrolyse the organometallic precursors to ZnO. The final nanoparticle suspension was precipitated by adding acetone, centrifuged and washed by toluene/acetone and acetone with subsequent centrifugation steps. The particles were air dried overnight. To halt any ripening which may occur in the solid state the particles were stored under N_2 gas or vacuum. Further details on nanoparticle preparation and characterisation are provided in the Supporting Information.

Preparation of polymer samples: Swelling solutions for incorporating oleate-capped ZnO nanoparticles into polyurethane were prepared by immersing polyurethane squares (1 cm^2) into a toluene suspension containing ZnO (1 mg/mL). The polymer samples were left to swell-encapsulate at room temperature for 24 h and then dipped into aqueous crystal violet solution in water (0.001 M) for 72 h in the dark. Control samples (treated with toluene only), ZnO-encapsulated polyurethane and CV-coated polyurethane were also prepared for the microbiology experiments.

Microbiological Investigation: The antibacterial activity of the treated polymer samples was tested against *Pseudomonas aeruginosa* NCTC 10662, *Staphylococcus aureus* NCTC 13143 which is representative of one of the two types of methicillin-resistant *S. aureus* that dominate in UK hospitals

(EMRSA-16),[2949] a clinical strain of methicillin-resistant *Staphylococcus aureus* (MRSA 4742; obtained from P. Wilson, University College London Hospital), a multidrug resistant strain of *Escherichia coli* positive for both NDM and OXA-48-like carbapenemase genes, *E. coli* 1030 (J. Wade, King's College Hospital, London) and endospores of *C. difficile* 630[37]. The following samples were used in the microbiological investigation: (i) solvent treated (control), (ii) ZnO-encapsulated polymer, (iii) crystal violet-coated polymer (CV) and (iv) CV and ZnO-encapsulated polymer.

P. aeruginosa NCTC 10662, *S. aureus* NCTC 13143, MRSA 4742 and *E. coli* 1030 were stored at -70 °C in Brain-Heart-Infusion broth (BHI, Oxoid) containing 20% (v/v) glycerol and propagated on either MacConkey agar (MAC, Oxoid) in the case of *P. aeruginosa* and *E. coli* or mannitol salt agar (MSA, Oxoid) in the case of *S. aureus*, for a maximum of two subcultures at intervals of two weeks.

BHI broth was inoculated with 1 bacterial colony and cultured in air with shaking (37 °C, 200 rpm, 18 h). The bacterial pellet was recovered by centrifugation, (20 °C , 2867.2 *g*, 5 min), washed in PBS (10 mL), centrifuged again to recover the pellet (20 °C, 2867.2 *g*, 5 min), and the bacteria were finally re-suspended in 10 ml of PBS. The washed suspension was diluted 1000-fold to achieve an inoculum of ~10^6 cfu/mL. In each experiment, the inoculum was confirmed by plating 10-fold serial dilutions on agar for viable counts. Triplicates of each polymer sample type were inoculated with 25 µL of the inoculum and incubated in the dark or irradiated for up to 6 hours using a white light source emitting an average light intensity of 500 lux.

After incubation, the inoculated samples were added to PBS (450 µL) and mixed using a vortex mixer (15 s). The neat suspension and 10-fold serial dilutions were plated on agar for viable counts and incubated aerobically at 37 °C for 24 h (*P. aeruginosa*/*E. coli*) or 48 hours (*S. aureus*). The experiment was repeated three times and the statistical significance of the following comparisons was analysed using the Mann-Whitney U test: (i) control polymer vs. inoculum; (ii) CV or ZnO vs. control, (iii) CV and ZnO vs. CV alone.

C. difficile spore preparation: C. difficile strains were grown at 37°C anaerobically in BHIS (Brain-Heart-Infusion supplemented with L-cysteine (0.1%; Sigma, UK). Sporulation of *C. difficile* was achieved using a method adapted from Burns *et al*.[48] 0.1% sodium taurocholate (Sigma, UK) was added to brain heart-infusion agar (BHI, Oxoid) to stimulate spore germination.

Superoxide and singlet oxygen detection: Superoxide dismutase (SOD) and L-histidine (Sigma-Aldrich, UK) were filter-sterilised and added to suspensions of *S. aureus* NCTC 13143 and *E. coli* ATCC 25922 to

determine the antibacterial mechanism of CVZnO-encapsulated polyurethane. SOD (50 U mL^{-1}) was used to eliminate superoxide, a precursor of hydrogen peroxide in radical formation, and L-histidine (1 mM) was added as a quencher of singlet oxygen ($^1O_2$). Furfuryl alcohol was used as a singlet oxygen probe by illuminating the modified samples suspended in furfuryl alcohol with the same visible light source and time conditions used in the microbiology investigation. The absorbance of this compound was measured at 222 nm from the control polymer and compared with CV- and CVZnO-incorporated polymer.[49]

Supporting Information

Supporting information includes methods for material preparation and characterisation and supporting results referred to in the main text. This information is available free of charge on the ACS Publications website.

Acknowledgements

S.S. would like to thank Dr. S. Sathasivam from UCL for his help with XPS, Dr A. Goode at Imperial College London for SEM analysis and UCL for the award of an Impact studentship. S.P. would like to thank Sheng Hu from ICL for her help with ICP-OES. S.N. would like to thank the Ramsay Memorial Fellowship Trust for the award of a fellowship.

References

(1) Reddy, K. M.; Feris, K.; Bell, J.; Wingett, D. G.; Hanley, C.; Punnoose, A. Selective Toxicity of Zinc Oxide Nanoparticles to Prokaryotic and Eukaryotic Systems. *Appl. Phys. Lett.* **2007**, *90* (21). https://doi.org/10.1063/1.2742324.

(2) Tayel, A. A.; El-Tras, W. F.; Moussa, S.; El-Baz, A. F.; Mahrous, H.; Salem, M. F.; Brimer, L. Antibacterial Action of Zinc Oxide Nanoparticles against Foodborne Pathogens. *J. Food Saf.* **2011**, *31* (2), 211–218. https://doi.org/10.1111/j.1745-4565.2010.00287.x.

(3) Fan, Q.; Yang, J.; Yu, Y.; Zhang, J.; Cao, J. Electronic Structure and Optical Properties of Al-Doped ZnO from Hybrid Functional Calculations. In *CHEMICAL ENGINEERING TRANSACTIONS*; 2015; Vol. 46. https://doi.org/10.3303/CET1546165.

(4) Sudha,M. Rajarajan, M. Deactivation of Photocatalytically Active ZnO Nanoparticle by Surface Capping with Poly Vinyl Pyrrolidone. *IOSR J. Appl. Chem.* **2013**, *3* (3), 45–53. https://doi.org/10.9790/5736-0334553.

(5) Xie, Y.; He, Y.; Irwin, P. L.; Jin, T.; Shi, X. Antibacterial Activity and Mechanism of Action of Zinc Oxide Nanoparticles against Campylobacter Jejuni. *Appl. Environ. Microbiol.* **2011**, *77* (7), 2325–2331. https://doi.org/10.1128/AEM.02149-10.

(6) Raghupathi, K. R.; Koodali, R. T.; Manna, A. C. Size-Dependent Bacterial Growth Inhibition and Mechanism of Antibacterial Activity of Zinc Oxide Nanoparticles. *Langmuir* **2011**, *27* (7), 4020–4028. https://doi.org/10.1021/la104825u.

(7) Sydnor, E. R. M.; Perl, T. M. Hospital Epidemiology and Infection Control in Acute-Care Settings. *Clin. Microbiol. Rev.* **2011**, *24* (1), 141–173. https://doi.org/10.1128/CMR.00027-10.

(8) Centers for Disease Control and Prevention. *Healthcare-Associated Infections*; 2016.

(9) Matsunaga, N.; Hayakawa, K. Estimating the Impact of Antimicrobial Resistance. *Lancet. Glob. Heal.* **2018**, *6* (9), e934–e935. https://doi.org/10.1016/S2214-109X(18)30325-5.

(10) Yoshikawa, T. T. Epidemiology and Unique Aspects of Aging and Infectious Diseases. *Clin. Infect. Dis.* **2000**, *30* (6), 931–933. https://doi.org/10.1086/313792.

(11) Hickson, M. Probiotics in the Prevention of Antibiotic-Associated Diarrhoea and Clostridium Difficile Infection. *Therap. Adv. Gastroenterol.* **2011**, *4* (3), 185–197. https://doi.org/10.1177/1756283X11399115.

(12) Khanna, S.; Pardi, D. S. Clostridium Difficile Infection: New Insights into Management. *Mayo Clinic Proceedings*. Elsevier Ltd November 2012, pp 1106–1117. https://doi.org/10.1016/j.mayocp.2012.07.016.

(13) World Health Organization. Hand Hygiene Technique with Soap and Water. In *WHO Guidelines on Hand Hygiene in Health Care*; 2009; p 156. https://doi.org/10.1086/600379.

(14) Sehmi, S. K.; Noimark, S.; Bear, J. C.; Peveler, W. J.; Bovis, M.; Allan, E.; MacRobert, A. J.; Parkin, I. P. Lethal Photosensitisation of Staphylococcus Aureus and Escherichia Coli Using Crystal Violet and Zinc Oxide-Encapsulated Polyurethane. *J. Mater. Chem. B* **2015**, *3* (31),

6490–6500. https://doi.org/10.1039/c5tb00971e.

(15) Noimark, S.; Dunnill, C. W.; Kay, C. W. M.; Perni, S.; Prokopovich, P.; Ismail, S.; Wilson, M.; Parkin, I. P. Incorporation of Methylene Blue and Nanogold into Polyvinyl Chloride Catheters; A New Approach for Light-Activated Disinfection of Surfaces. *J. Mater. Chem.* **2012**, *22* (30), 15388–15396. https://doi.org/10.1039/c2jm31987j.

(16) Moura, N. M. M.; Esteves, M.; Vieira, C.; Rocha, G. M. S. R. O.; Faustino, M. A. F.; Almeida, A.; Cavaleiro, J. A. S.; Lodeiro, C.; Neves, M. G. P. M. S. Novel β-Functionalized Mono-Charged Porphyrinic Derivatives: Synthesis and Photoinactivation of Escherichia Coli. *Dye. Pigment.* **2019**, *160*, 361–371. https://doi.org/10.1016/j.dyepig.2018.06.048.

(17) Perni, S.; Piccirillo, C.; Kafizas, A.; Uppal, M.; Pratten, J.; Wilson, M.; Parkin, I. P. Antibacterial Activity of Light-Activated Silicone Containing Methylene Blue and Gold Nanoparticles of Different Sizes. *J. Clust. Sci.* **2010**, *21* (3), 427–438. https://doi.org/10.1007/s10876-010-0319-5.

(18) Ozkan, E.; Allan, E.; Parkin, I. P. The Antibacterial Properties of Light-Activated Polydimethylsiloxane Containing Crystal Violet. *RSC Adv.* **2014**, *4* (93), 51711–51715. https://doi.org/10.1039/c4ra08503e.

(19) Hwang, G. B.; Allan, E.; Parkin, I. P. White Light-Activated Antimicrobial Paint Using Crystal Violet. *ACS Appl. Mater. Interfaces* **2016**, *8* (24), 15033–15039. https://doi.org/10.1021/acsami.5b06927.

(20) Ozkan, E.; Ozkan, F. T.; Allan, E.; Parkin, I. P. The Use of Zinc Oxide Nanoparticles to Enhance the Antibacterial Properties of Light-Activated Polydimethylsiloxane Containing Crystal Violet. *RSC Adv.* **2015**, *5* (12), 8806–8813. https://doi.org/10.1039/c4ra13649g.

(21) Noimark, S.; Weiner, J.; Noor, N.; Allan, E.; Williams, C. K.; Shaffer, M. S. P.; Parkin, I. P. Dual-Mechanism Antimicrobial Polymer-ZnO Nanoparticle and Crystal Violet-Encapsulated Silicone. *Adv. Funct. Mater.* **2015**, *25* (9), 1367–1373. https://doi.org/10.1002/adfm.201402980.

(22) Noimark, S.; Page, K.; Bear, J. C.; Sotelo-Vazquez, C.; Quesada-Cabrera, R.; Lu, Y.; Allan, E.; Darr, J. A.; Parkin, I. P. Functionalised Gold and Titania Nanoparticles and Surfaces for Use as Antimicrobial Coatings. *Faraday Discuss.* **2014**, *175* (0), 273–287. https://doi.org/10.1039/c4fd00113c.

(23) MacDonald, T. J.; Wu, K.; Sehmi, S. K.; Noimark, S.; Peveler, W. J.; Du Toit, H.; Voelcker, N. H.;

Allan, E.; MacRobert, A. J.; Gavriilidis, A.; et al. Thiol-Capped Gold Nanoparticles Swell-Encapsulated into Polyurethane as Powerful Antibacterial Surfaces under Dark and Light Conditions. *Sci. Rep.* **2016**, *6* (1), 39272. https://doi.org/10.1038/srep39272.

(24) Biel, M. A.; Sievert, C.; Usacheva, M.; Teichert, M.; Wedell, E.; Loebel, N.; Rose, A.; Zimmermann, R. Reduction of Endotracheal Tube Biofilms Using Antimicrobial Photodynamic Therapy. *Lasers Surg. Med.* **2011**, *43* (7), 586–590. https://doi.org/10.1002/lsm.21103.

(25) Mroz, P.; Yaroslavsky, A.; Kharkwal, G. B.; Hamblin, M. R. Cell Death Pathways in Photodynamic Therapy of Cancer. *Cancers*. June 2011, pp 2516–2539. https://doi.org/10.3390/cancers3022516.

(26) Chiaviello, A.; Postiglione, I.; Palumbo, G. Targets and Mechanisms of Photodynamic Therapy in Lung Cancer Cells: A Brief Overview. *Cancers (Basel).* **2011**, *3* (1), 1014–1041. https://doi.org/10.3390/cancers3011014.

(27) Allison, R. R.; Moghissi, K. Photodynamic Therapy (PDT): PDT Mechanisms. *Clin. Endosc.* **2013**, *46* (1), 24–29. https://doi.org/10.5946/ce.2013.46.1.24.

(28) Sehmi, S. K.; Noimark, S.; Pike, S. D.; Bear, J. C.; Peveler, W. J.; Williams, C. K.; Shaffer, M. S. P.; Allan, E.; Parkin, I. P.; MacRobert, A. J. Enhancing the Antibacterial Activity of Light-Activated Surfaces Containing Crystal Violet and ZnO Nanoparticles: Investigation of Nanoparticle Size, Capping Ligand, and Dopants. *ACS Omega* **2016**, *1* (3), 334–343. https://doi.org/10.1021/acsomega.6b00017.

(29) Das, S.; Anderson, C. J.; Grayes, A.; Mendoza, K.; Harazin, M.; Schora, D. M.; Peterson, L. R. Nasal Carriage of Epidemic Methicillin-Resistant Staphylococcus Aureus 15 (EMRSA-15) Clone Observed in Three Chicago-Area Long-Term Care Facilities. *Antimicrob. Agents Chemother.* **2013**, *57* (9), 4551–4553. https://doi.org/10.1128/AAC.00528-13.

(30) Nerandzic, M. M.; Cadnum, J. L.; Pultz, M. J.; Donskey, C. J. Evaluation of an Automated Ultraviolet Radiation Device for Decontamination of Clostridium Difficile and Other Healthcare-Associated Pathogens in Hospital Rooms. *BMC Infect. Dis.* **2010**, *10*, 197. https://doi.org/10.1186/1471-2334-10-197.

(31) Orchard, K. L.; Shaffer, M. S. P.; Williams, C. K. Organometallic Route to Surface-Modified ZnO Nanoparticles Suitable for in Situ Nanocomposite Synthesis: Bound Carboxylate Stoichiometry Controls Particle Size or Surface Coverage. *Chem. Mater.* **2012**, *24* (13), 2443–2448. https://doi.org/10.1021/cm300058d.

(32) Ali, M.; Winterer, M. ZnO Nanocrystals: Surprisingly “Alive.” *Chem. Mater.* **2010**, *22* (1), 85–91. https://doi.org/10.1021/cm902240c.

(33) Meulenkamp, E. A. Synthesis and Growth of ZnO Nanoparticles. *J. Phys. Chem. B* **1998**, *102* (29), 5566–5572. https://doi.org/10.1021/jp980730h.

(34) Silverwood, I. P.; Keyworth, C. W.; Brown, N. J.; Shaffer, M. S. P.; Williams, C. K.; Hellgardt, K.; Kelsall, G. H.; Kazarian, S. G. An Attenuated Total Reflection Fourier Transform Infrared (ATR FT-IR) Spectroscopic Study of Gas Adsorption on Colloidal Stearate-Capped ZnO Catalyst Substrate. *Appl. Spectrosc.* **2014**, *68* (1), 88–94. https://doi.org/10.1366/13-07174.

(35) Sehmi, S. K.; Noimark, S.; Weiner, J.; Allan, E.; MacRobert, A. J.; Parkin, I. P. Potent Antibacterial Activity of Copper Embedded into Silicone and Polyurethane. *ACS Appl. Mater. Interfaces* **2015**, *7* (41), 22807–22813. https://doi.org/10.1021/acsami.5b08665.

(36) Sehmi, S. Antibacterial Surfaces with Nanoparticle Incorporation for Prevention of Hospital-Acquired Infections. *Dr. thesis, UCL (University Coll. London).* **2016**.

(37) Sebaihia, M.; Wren, B. W.; Mullany, P.; Fairweather, N. F.; Minton, N.; Stabler, R.; Thomson, N. R.; Roberts, A. P.; Cerdeño-Tárraga, A. M.; Wang, H.; et al. The Multidrug-Resistant Human Pathogen Clostridium Difficile Has a Highly Mobile, Mosaic Genome. *Nat. Genet.* **2006**, *38* (7), 779–786. https://doi.org/10.1038/ng1830.

(38) Zheng, C. J.; Yoo, J. S.; Lee, T. G.; Cho, H. Y.; Kim, Y. H.; Kim, W. G. Fatty Acid Synthesis Is a Target for Antibacterial Activity of Unsaturated Fatty Acids. *FEBS Lett.* **2005**, *579* (23), 5157–5162. https://doi.org/10.1016/j.febslet.2005.08.028.

(39) Chandrasekaran, M.; Kannathasan, K.; Venkatesalu, V. Antimicrobial Activity of Fatty Acid Methyl Esters of Some Members of Chenopodiaceae. *Zeitschrift fur Naturforsch. - Sect. C J. Biosci.* **2008**, *63* (5–6), 331–336. https://doi.org/10.1515/znc-2008-5-604.

(40) Choi, J. S.; Park, N. H.; Hwang, S. Y.; Sohn, J. H.; Kwak, I.; Cho, K. K.; Choi, I. S. The Antibacterial Activity of Various Saturated and Unsaturated Fatty Acids against Several Oral Pathogens. *J. Environ. Biol.* **2013**, *34* (4), 673–676.

(41) Pal, S.; Tak, Y. K.; Song, J. M. Does the Antibacterial Activity of Silver Nanoparticles Depend on the Shape of the Nanoparticle? A Study of the Gram-Negative Bacterium Escherichia Coli. *Appl. Environ. Microbiol.* **2007**, *73* (6), 1712–1720. https://doi.org/10.1128/AEM.02218-06.

(42) Jeong, Y.; Lim, D. W.; Choi, J. Assessment of Size-Dependent Antimicrobial and Cytotoxic Properties of Silver Nanoparticles. *Adv. Mater. Sci. Eng.* **2014**, *2014* (September 2014).

https://doi.org/10.1155/2014/763807.

(43) Weiner, J.; Correia, A.; Peveler, W. J.; Kay, C. W. M.; Bovis, M. J.; Allan, E.; Woodhams, J. H.; Parkin, I. P.; Noimark, S.; MacRobert, A. J.; et al. Photosensitisation Studies of Silicone Polymer Doped with Methylene Blue and Nanogold for Antimicrobial Applications. *RSC Adv.* **2015**, *5* (68), 54830–54842. https://doi.org/10.1039/c5ra09045h.

(44) Ergaieg, K.; Chevanne, M.; Cillard, J.; Seux, R. Involvement of Both Type I and Type II Mechanisms in Gram-Positive and Gram-Negative Bacteria Photosensitization by a Meso-Substituted Cationic Porphyrin. *Sol. Energy* **2008**, *82* (12), 1107–1117. https://doi.org/10.1016/j.solener.2008.05.008.

(45) Li, Y.; Zhang, W.; Niu, J.; Chen, Y. Mechanism of Photogenerated Reactive Oxygen Species and Correlation with the Antibacterial Properties of Engineered Metal-Oxide Nanoparticles. *ACS Nano* **2012**, *6* (6), 5164–5173. https://doi.org/10.1021/nn300934k.

(46) Haag, W. R.; Hoigné, J.; Gassman, E.; Braun, A. M. Singlet Oxygen in Surface Waters - Part I: Furfuryl Alcohol as a Trapping Agent. *Chemosphere* **1984**, *13* (5–6), 631–640. https://doi.org/10.1016/0045-6535(84)90199-1.

(47) Kramarenko, G. G.; Hummel, S. G.; Martin, S. M.; Buettner, G. R. Ascorbate Reacts with Singlet Oxygen to Produce Hydrogen Peroxide. *Photochem. Photobiol.* **2006**, *82* (6), 1634–1637. https://doi.org/10.1562/2006-01-12-RN-774.

(48) Burns, D. A.; Heap, J. T.; Minton, N. P. SleC Is Essential for Germination of Clostridium Difficile Spores in Nutrient-Rich Medium Supplemented with the Bile Salt Taurocholate. *J. Bacteriol.* **2010**, *192* (3), 657–664. https://doi.org/10.1128/JB.01209-09.

(49) Allen, J. M.; Gossett, C. J.; Allen, S. K. Photochemical Formation of Singlet Molecular Oxygen (1O2) in Illuminated Aqueous Solutions of p-Aminobenzoic Acid (PABA). *J. Photochem. Photobiol. B Biol.* **1996**, *32* (1–2), 33–37. https://doi.org/10.1016/1011-1344(95)07185-7.

For table of contents only

Ambient Light
500 Lux

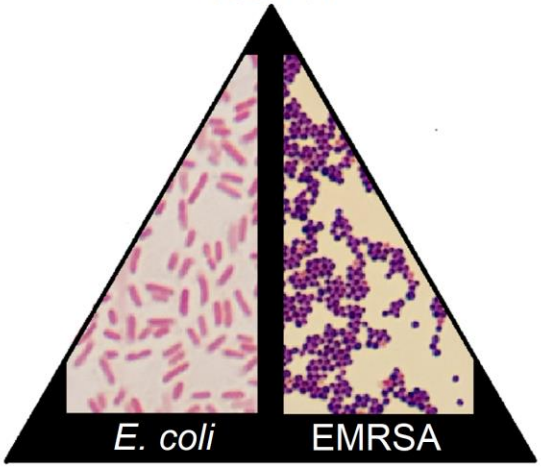

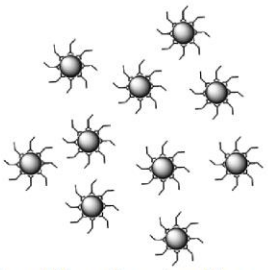

ZnO with oleate ligands
3.8 nm diameter

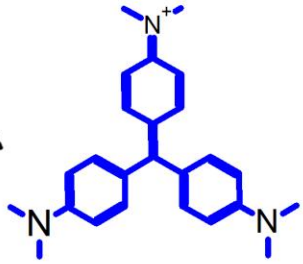

Crystal Violet